

Birth and evolution of an optical vortex

GIUSEPPE VALLONE,^{1,*} ANNA SPONSELLI,² VINCENZO D'AMBROSIO,^{3,5} LORENZO MARRUCCI,⁴ FABIO SCIARRINO³ AND PAOLO VILLORESI¹

¹*Dipartimento di Ingegneria dell'Informazione, Università di Padova, I-35131 Padova, Italy*

²*Dipartimento di Fisica e Astronomia, Università di Padova, I-35131 Padova, Italy*

³*Dipartimento di Fisica, Sapienza Università di Roma, I-00185 Roma, Italy*

⁴*Dipartimento di Fisica, Università di Napoli Federico II and CNR-ISASI Napoli, Italy*

⁵*Present address: ICFO-Institut de Ciències Fòniques, Barcelona Institute of Science and Technology, 08860 Castelldefels, Spain*

*vallone@dei.unipd.it

Abstract: When a phase singularity is suddenly imprinted on the axis of an ordinary Gaussian beam, an optical vortex appears and starts to grow radially, by effect of diffraction. This radial growth and the subsequent evolution of the optical vortex under focusing or imaging can be well described in general within the recently introduced theory of circular beams, which generalize the hypergeometric-Gaussian beams and which obey novel kinds of ABCD rules. Here, we investigate experimentally these vortex propagation phenomena and test the validity of circular-beam theory. Moreover, we analyze the difference in radial structure between the newly generated optical vortex and the vortex obtained in the image plane, where perfect imaging would lead to complete closure of the vortex core.

© 2016 Optical Society of America

OCIS codes: (070.2580) Paraxial wave optics; (070.7345) Wave propagation; (230.3720) Liquid-crystal devices.

References and links

1. J. F. Nye and M. V. Berry, "Dislocations in Wave Trains," *Proc. R. Soc. A* **336**, 165–190 (1974).
2. L. Allen, M. W. Beijersbergen, R. J. C. Spreeuw, and J. P. Woerdman, "Orbital angular momentum of light and the transformation of Laguerre-Gaussian laser modes," *Phys. Rev. A* **45**, 8185–8190 (1992).
3. M. Beijersbergen, R. Coerwinkel, M. Kristensen, and J. Woerdman, "Helical-wavefront laser beams produced with a spiral phaseplate," *Opt. Commun.* **112**, 321–327 (1994).
4. N. R. Heckenberg, R. McDuff, C. Smith, and A. G. White, "Generation of optical phase singularities by computer-generated holograms," *Opt. Lett.* **17**, 221–223 (1992).
5. L. Marrucci, C. Manzo, and D. Paparo, "Optical Spin-to-Orbital Angular Momentum Conversion in Inhomogeneous Anisotropic Media," *Phys. Rev. Lett.* **96**, 163905 (2006).
6. B. Piccirillo, V. D'Ambrosio, S. Slussarenko, L. Marrucci, and E. Santamato, "Photon spin-to-orbital angular momentum conversion via an electrically tunable q-plate," *Appl. Phys. Lett.* **97**, 241104 (2010).
7. V. D'Ambrosio, F. Baccari, S. Slussarenko, L. Marrucci, and F. Sciarrino, "Arbitrary, direct and deterministic manipulation of vector beams via electrically-tuned q-plates," *Sci. Rep.* **5**, 7840 (2015).
8. A. M. Yao and M. J. Padgett, "Orbital angular momentum: origins, behavior and applications," *Adv. Opt. Photon.* **3**, 161–204 (2011).
9. V. D'Ambrosio, E. Nagali, S. P. Walborn, L. Aolita, S. Slussarenko, L. Marrucci, and F. Sciarrino, "Complete experimental toolbox for alignment-free quantum communication," *Nat. Commun.* **3**, 961 (2012).
10. G. Vallone, V. D'Ambrosio, A. Sponselli, S. Slussarenko, L. Marrucci, F. Sciarrino, and P. Villoresi, "Free-Space Quantum Key Distribution by Rotation-Invariant Twisted Photons," *Phys. Rev. Lett.* **113**, 060503 (2014).
11. Z. S. Sacks, D. Rozas, and G. A. Swartzlander, Jr., "Holographic formation of optical-vortex filaments," *J. Opt. Soc. Am. B* **15**, 2226–2234 (1998).
12. S. Sundbeck, I. Gruzberg, and D. G. Grier, "Structure and scaling of helical modes of light," *Opt. Lett.* **30**, 477–479 (2005).
13. G. Vallone, G. Parisi, F. Spinello, E. Mari, F. Tamburini, and P. Villoresi, "A general theorem on the divergence of vortex beams," [arXiv:1601.02350] (2016).
14. V. V. Kotlyar, *et al.*, "Generation of phase singularity through diffracting a plane or Gaussian beam by a spiral phase plate," *J. Opt. Soc. Am. A* **22**, 849–861 (2005).
15. Greg Gbur, "Fractional vortex Hilbert's Hotel," *Optica* **3**, 222–225 (2016).
16. E. Karimi, *et al.*, "Hypergeometric-Gaussian modes," *Opt. Lett.* **32**, 3053–3055 (2007).
17. M. A. Bandres and J. C. Gutiérrez-Vega, "Circular beams," *Opt. Lett.* **33**, 177–179 (2008).

18. G. Vallone, "On the properties of circular beams: normalization, Laguerre Gauss expansion, and free-space divergence," *Opt. Lett.* **40**, 1717–1720 (2015).
19. A. E. Siegman, *Lasers*, (University Science, 1986).
20. E. Karimi, B. Piccirillo, L. Marrucci, and E. Santamato, "Improved focusing with Hypergeometric-Gaussian type-II optical modes," *Opt. Express* **16**, 21069–21075 (2008).
21. A. Y. Bekshaev, and A. I. Karamoch, "Spatial characteristics of vortex light beams produced by diffraction gratings with embedded phase singularity," *Opt. Commun.* **281**, 1366–1374 (2008).

1. Introduction

Research on the properties of optical vortices started with the seminal work of J. Nye and M. Berry [1]. There, the optical vortex was defined as a line along which the phase of the electromagnetic field is indeterminate, namely a line on which the intensity is zero. Beams carrying a defined photon value of the orbital angular momentum (OAM) are characterized by an optical vortex on the beam axis: the phase integration around the vortex divided by 2π gives an integer value, ℓ , corresponding to the OAM content of the beam (per photon).

The observation that Laguerre-Gaussian (LG) modes have a well-defined OAM [2] has prompted, in the last decades, the investigation of the properties of beams carrying OAM and the possible techniques to generate, manipulate and analyze them. Nowadays, several devices are used to generate OAM beams: spiral phase plates [3], diffractive elements such as holograms [4] or spiral Fresnel lenses, cylindrical lenses, spatial light modulators and q -plates [5–7] (see [8] for a general review on the devices used to generate OAM). Each of them, applied to a plane wave (or to a Gaussian beam), generates an optical vortex by multiplying the field by the phase profile $\exp(i\ell\phi)$, where ϕ is the angular coordinate along the plane transverse to the propagation. For ideally thin elements, this occurs with no other alterations of the beam field profile at the device output plane (sudden approximation). The study of the dynamic of an optical vortex has important applications in many fields, such as long distance free-space propagation [9, 10] or microscopy with OAM beams. The first study on the generation of an optical vortex [11] investigated the creation of filaments and the possibility of having vortex sizes two orders of magnitude smaller than the overall beam size. The propagation features of beams with OAM were studied in [12] and recently, a general theorem on the divergence of vortex beam was demonstrated [13]. In [14], the far-field intensity distribution obtained with plane waves or Gaussian beams impinging on a phase plate was derived, while [15] theoretically studied the propagation of a Gaussian beam on which a fractional vortex plate is applied. In [16], the Hypergeometric-Gaussian (HyGG) modes were introduced and it was shown that they can be obtained by applying the singular phase factor to a Gaussian-parabolic transmittance profile.

However, the different studies lack a comprehensive model for the vortex propagation through generic systems. Here we fill this gap by presenting an analytical model that quantitatively describes birth, evolution and closure of an optical vortex passing through an optical system that includes free space and two lenses. We also experimentally verified the validity of this model. The main tool that we use is the recently introduced family of Circular beams (CiBs) [17, 18], representing a very general solution of the paraxial wave equation with OAM. The use of CiBs is motivated by their simple transformation law under a generic ABCD optical system (see eq. (2)). Since many well known beams carrying OAM are CiBs with particular values of the beam parameters, the ABCD law can be also easily applied to them. Then, in the present work we experimentally demonstrate that the CiBs represent an optimal model for the study of the properties of optical vortices propagating through generic paraxial optical systems.

2. Circular beams

The Circular beams, that will be used to model the birth and evolution of an optical vortex, are here introduced. We define the beam propagation direction as the z axis and we use polar

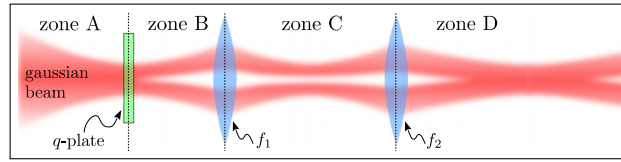


Fig. 1. Experimental setup. A Gaussian beam is sent through a q -plate that is placed at the beam waist location and generates the optical vortex. The obtained beam passes then through two lenses with focal lengths f_1 and f_2 . This defines three interesting propagation zones which will be analyzed: (B) newly generated vortex in free propagation; (C) focused vortex; (D) controlled imaging of the vortex source plane.

coordinates $\mathbf{x} = (r, \phi)$ in the plane transverse to the propagation. A generic CiB is determined by three complex parameters ξ , $q_0 := -d_0 + iz_0$ and p and one integer parameter $\ell \in \mathbb{Z}$. In a given transverse plane (say, $z = 0$), the monochromatic CiBs is defined as:

$$\text{CiB}_{p,\ell}^{(\xi,q_0)} = \mathcal{N} (1 + \xi \frac{q_0^*}{q_0})^{\frac{p}{2}} \left(\frac{i\sqrt{kz_0}r}{q_0} \right)^{|\ell|} G(r) {}_1F_1\left(-\frac{p}{2}, |\ell| + 1; \frac{r^2}{\chi^2}\right) e^{i\ell\phi}. \quad (1)$$

In the above equation $G(r) = i\sqrt{\frac{kz_0}{\pi}} e^{-\frac{ikr^2}{2q_0}} / q_0$ is the Gaussian beam, k is the wavevector, χ is defined by $\frac{1}{\chi^2} = \frac{kz_0\xi}{q_0} \frac{1}{q_0 + \xi q_0^*}$, ${}_1F_1$ is the Hypergeometric function and $\mathcal{N} = [|\ell|! {}_2F_1(-\frac{p}{2}, -\frac{p}{2}, |\ell| + 1, |\xi|^2)]^{-1/2}$ is a normalization factor depending on p , $|\ell|$ and $|\xi|$ [18].

We now give a physical interpretation of the parameters characterizing the CiBs. The first, ξ , is related to the “shape”: specific values of ξ identify some well-known beams. For instance, the limit $\xi \rightarrow +\infty$ corresponds to the standard LG modes [19]. CiBs with $|\xi| = 1$ correspond to the generalized HyGG [16, 18, 20]: in particular, the HyGG defined in [16] or the HyGG-II defined in [20] are obtained by setting $p \in \mathbb{R}$ and $\xi = 1$ or $\xi = -1$, respectively. We will show below that ξ is also related to the properties of the beam under the propagation through optical systems. The parameter q_0 is related to the physical scale (similarly to the complex beam parameter of the Gaussian beam [19]): its imaginary part is $z_0 = kw_0^2/2 > 0$ with w_0 the analog of the Gaussian “beam waist” while d_0 represents the location of the beam waist. Finally, p defines the radial index and ℓ corresponds to the carried OAM.

CiBs were originally defined [17] in terms of (q_0, q_1) , with $q_1 = \frac{q_0 + \xi q_0^*}{1 + \xi}$. However, the formulation in terms of (q_0, ξ) gives a clearer view when the propagation in free space and throughout a generic ABCD system is studied. In particular, as we will show, the parameter $|\xi|$ defines a “class” of beams with similar features under the propagation through generic optical systems. As derived in [17], the field resulting after a propagation along a distance d can be obtained from (1) by the transformation $q_j \rightarrow q_j + d$ with $j = 0, 1$. Such law is generalized for generic ABCD optical system in terms of (q_0, q_1) as $q_j \rightarrow (Aq_j + B)/(Cq_j + D)$, with $A, B, C, D \in \mathbb{R}$ [17]. By using (q_0, ξ) as beam parameters, the ABCD transformation can be rewritten as follows:

$$q_0 \rightarrow \frac{Aq_0 + B}{Cq_0 + D}, \quad \xi \rightarrow \frac{Cq_0^* + D}{Cq_0 + D} \xi. \quad (2)$$

It is worth noticing that, by the above transformation, the absolute value of ξ and the normalization \mathcal{N} are invariant. Then, the parameter $|\xi|$ identifies an “equivalence class” of CiBs under generic ABCD optical transformations: beams with different $|\xi|$'s cannot be obtained as input and output of any real ABCD system. Moreover, as noticed in [18], the value of the parameter $|\xi|$ determines the constraints on p to achieve square integrability. When $|\xi| < 1$ the beam is square integrable $\forall p$; when $|\xi| = 1$ it is required that $\Re(p) > -1 - |\ell|$; when $|\xi| > 1$ square

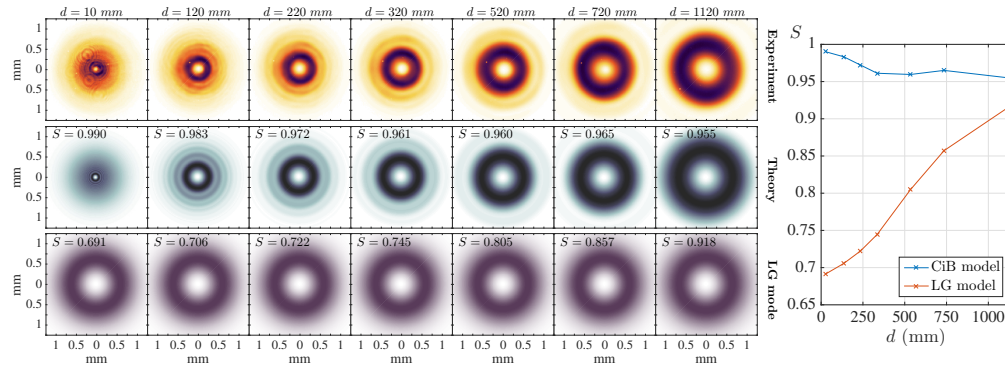


Fig. 2. “Birth” of the optical vortex. In the first row we show the experimental intensity patterns obtained after the q -plate placed at the beam waist location at various propagation distances d . The data should be compared with the theoretical CiB model shown in the second row. In the third row we show the corresponding Laguerre-Gauss mode with the same z_0 and beam waist located at $d = 0$. The degree of agreement between the two models and the experiment is measured by the reported similarity values, S , given in each panel and shown in the right inset for different values of d .

integrability imposes $p/2 \in \mathbb{N}$. Finally, ξ does not change in free-space propagation. Then, we believe that the description of CiBs in terms of (q_0, ξ) offers a clearer view of their properties during generic optical transformations.

The beams that can be easily experimentally generated by using phase plates or q -plates correspond to CiBs with $|\xi| = 1$: indeed, by applying the phase factor $e^{i\ell\phi}$ to a Gaussian beam with a given z_0 at a distance Δ from its waist plane, the CiBs with $\xi = \frac{z_0 - i\Delta}{z_0 + i\Delta}$ and $p = -|\ell|$ is generated [16, 18]. After straightforward calculations from (1), such beams can be written as:

$$\text{CiB}_{-|\ell|, \ell}^{(\xi, q_0)} = \frac{\Gamma(|\ell|/2 + 1)}{|\ell|!} \left(\frac{-r^2}{\xi\chi^2}\right)^{\frac{|\ell|}{2}} G(r) {}_1F_1\left(\frac{|\ell|}{2}, |\ell| + 1; \frac{r^2}{\chi^2}\right) e^{i\ell\phi}, \quad \text{when } |\xi| = 1. \quad (3)$$

The beam in (3), that carries ℓ units of OAM, is quite different from one of the well known (and very much used) $\text{LG}_{0, \ell}$ mode. Indeed, the intensity of a $\text{LG}_{0, \ell}$ mode presents an intensity pattern that has always an hole in the center, even at its waist location, while in the beam of eq. (3) the vortex is absent at a distance Δ from its waist plane, but starts to grow during propagation. The goal of our experiment is then to study the evolution of a beam generated by applying the phase $e^{i\ell\phi}$ to a Gaussian beam and to compare it with the CiB model.

3. The experiment

The experimental setup is shown in Fig. 1. A circular polarized Gaussian beam impinges on a q -plate placed on the beam waist. The optical vortex is then generated (the same results could be obtained with any device able to imprint the phase profile $e^{i\ell\phi}$). The obtained beam propagates through an optical system composed of two lenses with focal lengths f_1 and f_2 respectively. We measured the intensity pattern of the beam by a CCD camera across four different zones, labeled as A, B, C and D (Fig. 1), and compared the results with the model provided by the CiBs. As a reference, we first measured the properties of the impinging Gaussian beam at wavelength 810 nm without q -plate. Taking $z = 0$ the location of the beam waist, we measured the beam intensity at seven different distances d , ranging from 10 cm to 1120 cm . From them we derived the beam waist $w_0 = 850 \pm 10 \text{ } \mu\text{m}$, corresponding to a Rayleigh distance $z_0 = 2.80 \pm 0.07 \text{ m}$. To compare the theoretical and experimental intensity patterns we used the *similarity*, defined

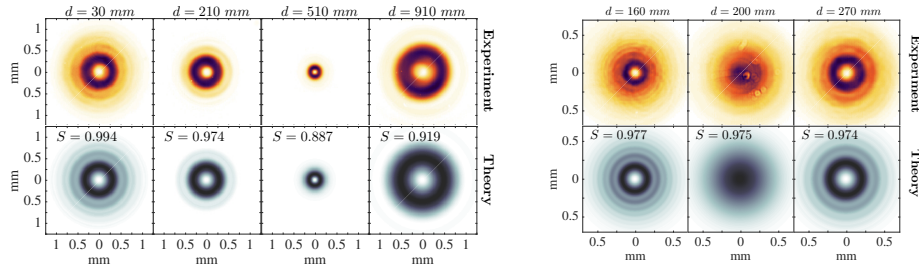


Fig. 3. **Left:** Focusing of an optical vortex by a lens. Experimental (upper row) and theoretical (lower row) intensity patterns obtained at various distances d from the focusing lens. **Right:** Quasi-closure of the optical vortex occurring when a real image of the vortex source is created by a lens system. Experimental (upper row) and theoretical (lower row) intensity patterns obtained at various distances d from the second lens. The medium panel for $d = 200$ mm corresponds to the image plane.

as $S = (\sum_{x,y} I_{x,y}^{\text{th}} I_{x,y}^{\text{exp}}) / \sqrt{\sum_{x,y} (I_{x,y}^{\text{th}})^2 \times \sum_{x,y} (I_{x,y}^{\text{exp}})^2}$ where $I_{x,y}^{\text{exp}}$ and $I_{x,y}^{\text{th}}$ are the experimental and theoretical intensities at point (x, y) respectively. In all the cases we measured $S > 0.98$.

We then placed a q -plate with $q = 1/2$ at the beam waist location, to observe the “birth” of the optical vortex: this corresponds to the “zone B” of Fig. 1. As predicted by the CiBs model, the vortex, related to the phase singularity on the beam axis, starts growing after the q -plate. After the propagation across a small distance, of the order of $z_0/10$, the vortex diameter stabilizes to a size of the order of half beam diameter. The “birth” of the optical vortex is shown in Fig. 2, where we compare the experimental intensity patterns with the theoretical model of (3) with $\ell = 1$, $\xi = 1$ and $q_0(d) = d + iz_0$. The good agreement between observed intensities and the predictions is proved by the similarities, always greater than 0.95: we here stress that that no fitting parameter was employed in the theoretical model. Indeed, we used as Rayleigh distance the value $z_0 = 2.8$ m obtained in the previous measurement. The parameter d reported in the top of Fig. 2 corresponds to the measured distance from the q -plate. In Fig. 2 we also show the intensity of a LG mode with $p = 0$, $\ell = 1$ and the same $z_0 = 2.8$ m, to demonstrate the differences between the experimental generated beam, its theoretical model represented by the CiBs and the widely used LG approximation. While the beam resembles a Laguerre-Gauss mode in the far field, in the near field (up to a distance of $\sim z_0/10$ from the q -plate) the LG approximation fails to correctly model the beam properties, as quantified by the low values of the similarities. In particular, the “birth” of the optical vortex cannot be modeled by a LG mode, since, for such beams, the vortex is present along all transverse planes during propagation, as shown for instance by the LG intensity patterns at $d = 10$ mm in Fig. 2. The same conclusions were obtained in the theoretical analysis of [21]: indeed, it is worth noticing that the subclass of CiB with $\xi = 1$ and $p = -|\ell|$ corresponds to the “Kummer beams” defined in [21]. However, the formulation in terms of CiBs, allows for a complete study of the propagation through generic optical systems, as we now demonstrate. Indeed, we also measured the beam evolution after a lens with focal length $f_1 = 510$ mm, corresponding to the “zone C” of Fig. 1. The lens was placed at distance $d_1 = 150$ mm from the q -plate plane and now we indicate by d the distance from the lens. By the ABCD law, the beam parameters $(q_0(d), \xi_C)$ in zone C can be calculated from $(iz_0, 1)$ by the matrix $M = \begin{pmatrix} 1-d/f_1 & d+d_1-dd_1/f_1 \\ -1/f_1 & 1-d_1/f_1 \end{pmatrix}$, obtaining

$$q_0(d) = \frac{(d+d_1)f_1 - dd_1 + iz_0(f_1 - d)}{f - d_1 - iz_0}, \quad \xi_C = \frac{f_1 - d_1 + iz_0}{f_1 - d_1 - iz_0}. \quad (4)$$

In zone C, as expected, ξ_C does not depend on d . We show the comparison between the measured

and calculated intensity patterns obtained at different distances d from the lens in the left panel of Fig. 3. The theoretical intensity patterns were evaluated by inserting in the CiBs of (3) the above values of $q_0(d)$ and $\xi(d)$. Four of the eight measured patterns and the corresponding similarities S are shown (the lowest of the eight measured similarity is 0.885): they demonstrate that CiB correctly models the propagation of such beam. We notice that the chosen position of the lens is such that no real imaging of the q -plate takes place in zone C.

We finally observed the beam in the “zone D”, that is after a second lens leading to the formation of a real image of the q -plate vortex source. In this case we used $f_1 = 300 \text{ mm}$ and $f_2 = 200 \text{ mm}$, with the lens f_1 placed at distance $d_1 = f_1$ from the q -plate and the lens f_2 placed at distance $f_1 + f_2$ from the first lens. We now indicate by d the distance after the lens f_2 . The ABCD matrix in this case is given by $M = \begin{pmatrix} -f_2/f_1 & f_1 - d f_1/f_2 \\ 0 & -f_1/f_2 \end{pmatrix}$ corresponding to $q_0(d) = d - f_1 + i z_0 f_2^2 / f_1^2$ and $\xi_D = 1$. In Fig. 3 (right) we show three of the seven measured patterns and the corresponding similarities S (now the lowest measured similarity was 0.928). It is worth noticing the almost complete closure of the vortex: at the plane $d = 200 \text{ mm}$ the vortex at the center almost completely disappears, even if the OAM content is still non-vanishing. The disappearance is actually not complete: a more accurate analysis (to be reported elsewhere) shows that the vortex radius reduces to a minimum value that depends on the numerical aperture of the optical imaging system, according to the standard resolution limits imposed by wave theory. However, this minimum vortex size can easily be orders of magnitude smaller than the beam size in the same plane. We further notice that an approximate theory based on LG vortex beams does not describe properly this vortex imaging phenomenon.

4. Conclusions

We have studied the generation and the propagation of an optical vortex created by superimposing an azimuthal phase pattern imprinted by a q -plate on a Gaussian beam. The application of such a phase mask is the principle on which all current approaches to generate and measure OAM eigenstates (spiral phase plates, fork holograms, q -plates) are based. By using an optical system with two lenses, we have experimentally verified for the first time the recently introduced ABCD law for Circular beams [17]. Our results demonstrate that the CiBs are very useful to analytically model the propagation through a generic optical system of OAM beams. We stress that many well known beams carrying OAM are included in the CiB family with particular values of the beam parameters. The accuracy of the q -plate in the generation of the singular phase profile $\exp(i\ell\phi)$ to the beam was essential to generate a highly stigmatic beam that perfectly matches the theoretical predictions.

Acknowledgments

Our work was supported by the Progetto di Ateneo PRAT 2013 (CPDA138592) of the University of Padova and by the ERC-Starting Grant 3D-QUEST (3D-Quantum Integrated Optical Simulation; grant agreement no. 307783): <http://www.3dquest.eu>. LM acknowledges support of the ERC-Advanced grant PHOSPhOR (grant agreement No. 694683)